Adsorption of Methane, Ethane, and Ethylene on Titanosilicate ETS-10 Zeolite

Nadhir A. Al-Baghli* and Kevin F. Loughlin†

Chemical Engineering Department, King Fahd University of Petroleum & Minerals, Dhahran, Saudi Arabia 31261

Equilibrium adsorption data are reported for methane, ethane, and ethylene on titanosilicate ETS-10 zeolite for pressures up to 1000 kPa and temperatures of (280, 300, 315, 325, and 350) K. The data are modeled using Toth, unilan, and virial three-constant isotherms. Unconstrained and constrained optimization techniques have been applied to derive the model parameters. Henry's constant and limiting enthalpies of adsorption are deduced from the virial three-constant model and compared to the values derived for the Toth and unilan models. The saturation concentration is deduced on the basis of the assumption of 95% occupancy of the free zeolite voidage with adsorbed-state molecular volumes estimated from liquid densities.

Introduction

Titanosilicate ETS-10, an experimental titanium silicate, was first synthesized in 1990.[1] It is a microporous crystalline solid consisting mainly of an assemblage of titanium oxide (TiO_2) and silicate (SiO_2). The pore sizes in titanosilicate ETS-10 are uniform and similar in dimension to large-pore classical zeolites. Titanium is octahedrally coordinated in the framework and requires two counterbalancing cations per titanium. The titanium atoms are ordered in two perpendicular linear chains in the $x-y$ plane and displaced by half a unit cell in the z direction. The chains are linked together by silica tetrahedra. The effective pore size of ETS-10 is about 8 Å, and it is thermally stable in air up to 600 °C. The properties of titanosilicate ETS-10 are presented in Table 1.[1]

Titanium zeolites such as ETS-4 and titanosilicate ETS-10 are extensively used in ion exchange, gas separation or purification, and catalytic studies. Studies have been reported by Gervasini et al.,[2,3] Bianchi et al.,[4,5] and Carniti et al.[6] The properties of these adsorbents were originally expounded on by Kuznicki et al.[1] and have being further examined by Pavel et al.[7,8] X-ray diffraction, UV−vis, NMR, EPR, and Raman studies have been used to characterize these zeolites in original or ion-exchanged forms by Zibrowius et al.,[9] Otero Arean et al.,[10] Anderson et al.,[11] Grillo and Carrazza,[12,13] Yang and Truitt,[14] Kishiman and Okubo,[15] Sankar et al.,[16] and Ashtekar et al.[17] The limited adsorption studies reported involve the adsorption of H_2, N_2, CO, NO, and O_2 on sodium and potassium titanosilicates,[18] pure component adsorption on titanosilicate ETS-10,[19] and the use of methane as a probe molecule for basic site determination.[20] Unlike other zeolites, strong framework deformations occur upon the adsorption of guest molecules.[17] Kuznicki et al.[21] have used this property to adjust the pore sizes of ETS-4 through systematic dehydration at elevated temperatures to "tune" the effective pores of the crystal. This can be successfully applied to tailor these adsorbents to give size-selective adsorbents for commercially important separations of gas mixtures of similar size in the 3 to 4 Å range, such as N_2-CH_4, $Ar-O_2$, and N_2-O_2.

Table 1. Properties of Titanosilicate ETS-10 Zeolites[1]

chemical composition	66.1% SiO_2, 17.4% TiO_2, 10.0% Na_2O, 4.8% K_2O, 1.7% others
ion exchange capacity	∼4.0 mequiv/g (as shipped hydrous) good stability for exchange in acidic media
moisture content (as shipped)	∼15 mass %
surface area	300+ $m^2 \cdot g^{-1}$
kinetic diameter	8 Å
stability	stable in air up to 600 °C
pore volume (as synthesized)	0.1195 $cm^3 \cdot g^{-1}$
structure	three-dimensional network of interconnecting channels intersecting at the center pore

The objective of the current study is to determine the adsorption behavior of pure methane, ethane, and ethylene on titanosilicate ETS-10 zeolite. The data are analyzed using Toth, unilan, and virial isotherms. Henry's constant and isosteric enthalpies of adsorption are deduced from the fit of these models to the data.

Theoretical Background

The equilibrium relationship in physical adsorption is highly affected by the characteristics of the adsorbents. For pure components and specified adsorbents, this relation is governed by the system temperature and pressure. At low pressure, the loading q (mol·kg^{-1}) is linearly related to the system pressure P (kPa) by

$$\lim_{P \to 0} q = K_H \times P \tag{1}$$

The coefficient K_H is known as Henry's constant (mol·kg^{-1}·kPa^{-1}) and is related to temperature by an Arrhenius-type equation

$$K_H = K_o \exp\left(\frac{-\Delta H}{RT}\right) \tag{2}$$

where K_o is a constant, the preexponential factor (mol·kg^{-1}·

* To whom correspondence should be addressed. E-mail: nabaghli@kfupm.edu.sa. Fax: 00966 (3) 860-4234.
† E-mail: loughkf@kfupm.edu.sa.

10.1021/je0496793 CCC: $30.25
Published on Web 04/19/2005

kPa^{-1}), $-\Delta H$ is the isosteric enthalpy of adsorption ($kJ \cdot mol^{-1}$), T is the temperature (K), and R is the universal gas constant ($kJ \cdot mol^{-1} \cdot K^{-1}$). Any thermodynamically consistent model should satisfy eq 1 at very low pressure.

In the upper limit, the pressure at which the pores are completely filled is the saturation pressure P_s (kPa), and the corresponding loading is the saturation concentration q_s defined as

$$\lim_{P \to P_s} q = q_s \tag{3}$$

The saturation concentration and Henry's constant are important physical parameters of any thermodynamically consistent model. The fraction of surface covered with adsorbed molecules θ is defined as

$$\theta = \frac{q}{q_s} \tag{4}$$

The saturation concentration can be theoretically calculated for microporous zeolites[22] by

$$q_s = \frac{\epsilon}{v^*} \tag{5}$$

where ϵ is the voidage of the adsorbent (119.5 $cm^3 \cdot kg^{-1}$ for titanosilicate ETS-10 zeolite (Table 1)) and v^* is the molar volume ($cm^3 \cdot mol^{-1}$) at the system temperature T given by[23]

$$v^* = v_b + \left[\frac{T - T_b}{T_c - T_b}\right](b - v_b) \tag{6}$$

where T_c and T_b are the critical and boiling point temperatures respectively (K), and v_b ($cm^3 \cdot mol^{-1}$) and b ($cm^3 \cdot mol^{-1}$) are the molar volume at T_b and the van der Waal's volume, respectively. Above the critical temperature, v^* is assumed equal to b. The values of the saturation concentration calculated from the above expressions are based on the assumption of complete occupancy of the free voidage with adsorbed molecules assumed to be analogous to a highly compressed liquid state under the same conditions. However, the actual value is frequently a little less because of steric effects.

Of the 10 models examined in the thesis of Al-Baghli,[24] only three are reported here. The reason for the selection of the 3 models reported (out of the 10 studied) is that they gave the most physically realistic and consistent values of the parameters, particularly the values of K_H, q_s, and $-\Delta H$. The three models selected are the Toth, unilan, and virial three-constant models.

Toth[25] derived a model based on monolayer adsorption, taking into account the heterogeneity of the adsorbent where the energies of the sites are no longer equivalent:

$$q = \frac{q_s P}{(b + P^t)^{1/t}} \tag{7}$$

where t is a heterogeneity parameter (dimensionless) and b is an equilibrium parameter (kPa^t) This model reduces to the Langmuir model for $t = 1$, which refers to a homogeneous surface. Applying eq 1 to Toth's model, we get

$$K_H = q_s b^{-1/t} \tag{8}$$

Honig and Reyerson[26] have developed a model based on a uniform distribution of energies of adsorption. The model is a modified version of the Langmuir model called the unilan model:

$$q = \frac{q_s}{2s} \ln\left[\frac{c + P \exp(s)}{c + P \exp(-s)}\right] \tag{9}$$

where c is an equilibrium parameter (kPa) and s is a dimensionless constant related to the heterogeneity of the surface. For a homogeneous surface, s vanishes, and the unilan model reduces to the Langmuir model. Henry's constant can be obtained from

$$K_H = \frac{q_s}{cs} \sinh(s) \tag{10}$$

The Gibbs adsorption isotherm may also be used in conjunction with an equation of state of the virial form

$$\frac{\pi A}{qRT} = 1 + B_1 q + B_2 q^2 + \cdots \tag{11}$$

to obtain the virial adsorption isotherm[27]

$$P = \frac{q}{K_H} \exp(A_1 q + A_2 q^2 + \cdots) \tag{12}$$

This isotherm does not give information about the nature of the adsorbed phase; therefore, it may be considered to be correlative.

However, this isotherm possesses a unique property in that it is independent of the saturation loading. The values of Henry's constant calculated from this model are thus totally independent of the saturation loading and consequently are deemed to be more accurate than models that include this parameter. Models inclusive of Henry's constant and the saturation loading seem to possess an interaction property that makes the calculation of either parameter inaccurate.

In this paper, the isotherm equations of the Toth, unilan, and virial models are used to model the experimental data. Model parameters are obtained using the nonlinear least-squares method

$$\text{ss} = \sum_{i=1}^{N} \left(\frac{q_{\text{mod}}}{q_{\text{expt}}} - 1\right)^2 \tag{13}$$

where ss is the sum-of-squares error, N is the number of data points, and q_{mod} and q_{expt} are the amount adsorbed per unit mass of adsorbent calculated from the model and experiment, respectively.

Both constrained and unconstrained optimizations have been applied for each model. In the unconstrained regression, the saturation concentration parameter q_s is obliged to be greater than the highest experimental concentration obtained at the highest pressure and lowest temperature, and the remaining parameters are left to relax to their optimum values. However, in the constrained regression, the saturation concentration parameter is fixed equal to 95% of the theoretical value calculated from eq 5, taking into consideration steric effects in the cavities. In addition, the parameters for each model that give similar values at different temperatures have been fixed to be constant at values that minimize the total sum-of-squares error. In the virial model, only the virial first constant has been fixed to be constant.

Experimental Procedure

The volumetric method is used to collect the adsorption data for all of the systems studied. Crystals of titanosilicate

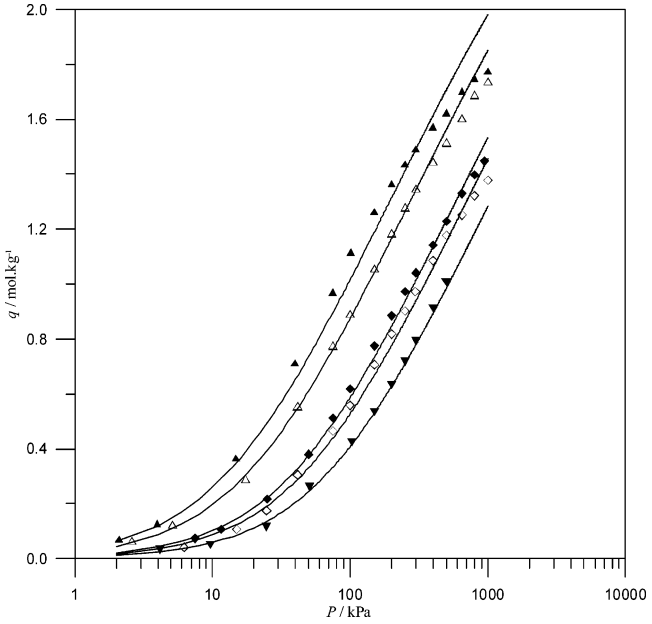

Figure 1. Fit of the unilan model to the isotherms of methane on titanosilicate ETS-10: ▲, 280 K; △, 300 K; ◆, 315 K; ◇, 325 K; ▼, 350 K.

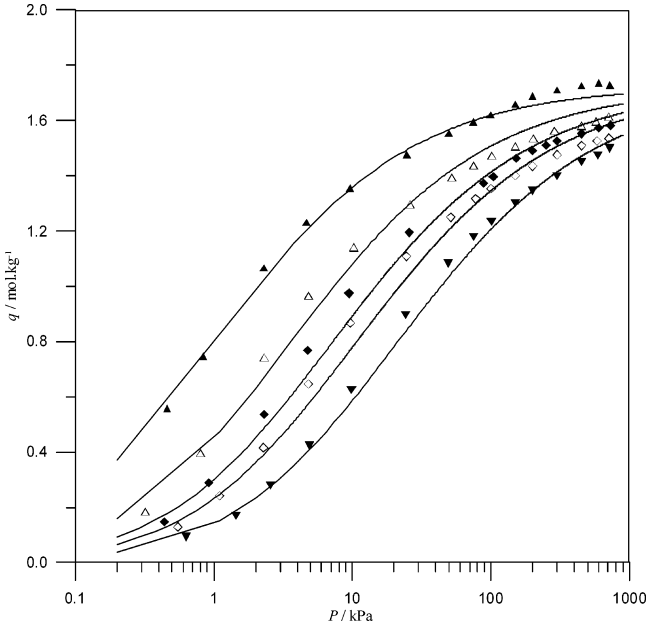

Figure 2. Fit of the Toth model to the isotherms of ethane on titanosilicate ETS-10: ▲, 280 K; △, 300 K; ◆, 315 K; ◇, 325 K; ▼, 350 K.

ETS-10 were obtained from Kuznicki[28] of Engelhard, New Jersey, and were extruded in the Research Institute at King Fahd University of Petroleum & Minerals using a negligible amount of Ludox 40 solution for binding. These were placed in the apparatus used by Abdul Rehman et al.[29,30] The experimental procedure followed is reported therein. The properties of the titanosilicate ETS-10 used are the same as those presented in Table 1.

Results and Discussion

X-ray diffraction analysis of the extruded titanosilicate ETS-10 sample indicated that the amount of noncrystalline material is negligible. This conclusion was also supported by the experimental values of q_s obtained for methane, ethane, and ethylene, which were very close to the theoretical values calculated for pure titanosilicate ETS-10 zeolite using eq 5.

The raw data for the adsorption of methane, ethane, and ethylene on titanosilicate ETS-10 zeolite are given in the Supporting Information. Five isotherms are reported for each gas, and an extra isotherm was measured at one of the temperatures to ascertain the reproducibility of the data. It was observed that the worst reproducibility was within 2%. The data and the fits of the unilan, Toth, and virial three-constant model are plotted in Figures 1−3, respectively. Because the data are measured using the volumetric method,[29] the experimental error in the calculated amount adsorbed, q, accumulates such that the last measured point is the least accurate. For example, the data for methane at high pressures deviate largely from the prediction of the unilan model as shown in Figure 1.

Unconstrained optimization parameters for the sorption of methane, ethane, and ethylene on titanosilicate ETS-10 zeolite are analyzed initially. The unconstrained optimization procedure revealed that the saturation concentration q_s in the Toth and unilan models varied significantly for the different isotherm temperatures, giving unacceptable values. The theoretical values of the saturation parameter q_s for methane, ethane, and ethylene in titanosilicate ETS-10 zeolite using eq 5 are 2.66, 1.75, and 2.00 mol·kg^{-1}, respectively. The unconstrained q_s values for the

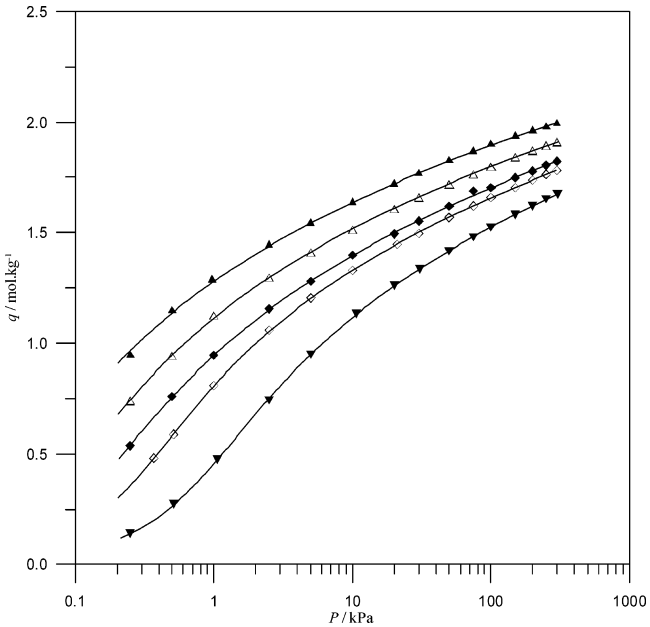

Figure 3. Fit of the virial three-constant model to the isotherms of ethylene on titanosilicate ETS-10: ▲, 280 K; △, 300 K; ◆, 315 K; ◇, 325 K; ▼, 350 K.

unilan model for ethylene ranged from 4.058 mol·kg^{-1} at 280 K to 3.883 mol·kg^{-1} at 350 K. These values are practically twice the theoretical limit of 2.00 mol·kg^{-1} and are unacceptable. There was also a strong interaction between Henry's constant K_H and the saturation concentration q_s parameters. For the virial isotherm, this interaction is nonexistent because there is no saturation concentration in this model. Accordingly, the variation of the K_H values between the different isotherms for the virial model is much lower than for the other two models. On the basis of this reasoning, we elected to pursue constrained optimization based on sound physical principles.

The pore volume of titanosilicate ETS-10 is 110 cm^3·kg^{-1}, which is less than 50% of that for the A-type zeolite (274 cm^3·kg^{-1}, Breck[22]). For the A zeolite, the volume occupied at saturation is 252, 213, 261, 226, and 230 cm^3·kg^{-1} for

Table 2. Constrained Optimization Parameters

methane Toth model[a]					
T/K	280	300	315	325	350
ss	0.0803	0.0227	0.0368	0.1553	0.0699
b/kPa^t	10.92	13.30	20.63	22.99	29.34
K_H/mol·kg^{-1}·kPa^{-1}	0.0431	0.0307	0.0144	0.0119	0.0078

methane unilan model[b]					
T/K	280	300	315	325	350
ss	0.0898	0.0331	0.0175	0.0899	0.0569
c/kPa	207.27	291.60	625.95	748.05	1114.32
K_H/mol·kg^{-1}·kPa^{-1}	0.0341	0.0242	0.0113	0.0094	0.0063

methane virial three-constant model[c]					
T/K	280	300	315	325	350
ss	0.0095	0.0477	0.0007	0.0275	0.0569
A_2/kg^2·mol^{-2}	0.0000	0.2250	0.2830	0.1950	0.5190
A_3/kg^3·mol^{-3}	0.3160	0.1420	0.1590	0.2590	0.0000
K_H/mol·kg^{-1}·kPa^{-1}	0.0306	0.0203	0.0100	0.0083	0.0057

ethane Toth model[d]					
T/K	280	300	315	325	350
ss	0.0060	0.0618	0.0541	0.0573	0.0236
b/kPa^t	0.571	1.169	1.733	2.172	3.207
K_H/mol·kg^{-1}·kPa^{-1}	4.681	1.331	0.667	0.449	0.227

ethane unilan model[e]					
T/K	280	300	315	325	350
ss	0.0228	0.1584	0.4282	0.1881	0.1737
c/kPa	1.368	5.181	7.205	14.140	27.641
K_H/mol·kg^{-1}·kPa^{-1}	5.068	1.338	0.962	0.490	0.251

ethane virial three-constant model[f]					
T/K	280	300	315	325	350
ss	0.0266	0.0217	0.0098	0.0106	0.0279
A_2/kg^2·mol^{-2}	0.000	0.000	0.000	0.000	0.099
A_3/kg^3·mol^{-3}	1.040	1.095	1.040	1.032	0.881
K_H/mol·kg^{-1}·kPa^{-1}	2.218	0.691	0.379	0.256	0.120

ethylene Toth model[g]					
T/K	280	300	315	325	350
ss	0.0217	0.0104	0.0427	0.0191	0.1783
b/kPa^t	0.203	0.290	0.369	0.369	0.899
K_H/mol·kg^{-1}·kPa^{-1}	88.956	38.170	21.433	10.259	2.574

ethylene unilan model[h]					
T/K	280	300	315	325	350
ss	0.0136	0.0244	0.0846	0.0809	1.2085
c/kPa	0.299	0.758	1.340	2.795	8.939
K_H/mol·kg^{-1}·kPa^{-1}	99.279	39.145	22.147	10.619	3.321

ethylene virial three-constant model[i]					
T/K	280	300	315	325	350
ss	0.0008	0.0001	0.0001	0.0001	0.0004
A_2/kg^2·mol^{-2}	0.000	0.092	0.305	0.035	0.263
A_3/kg^3·mol^{-3}	0.858	0.847	0.782	0.890	0.739
K_H/mol·kg^{-1}·kPa^{-1}	10.907	5.436	3.102	1.643	0.584

[a] t is constrained at 0.580, and q_s is constrained at 2.66 mol·kg^{-1}. [b] s is constrained at 2.650, and q_s is constrained at 2.66 mol·kg^{-1}. [c] A_1 is constrained at 0.550 kg·mol^{-1}. [d] t is constrained at 0.570, and q_s is constrained at 1.75 mol·kg^{-1}. [e] s is constrained at 3.25, and q_s is constrained at 1.75 mol·kg^{-1}. [f] A_1 is constrained at 0.480 kg·mol^{-1}. [g] t is constrained at 0.420, and q_s is constrained at 2.00 mol·kg^{-1}. [h] s is constrained at 5.00, and q_s is constrained at 2.00 mol·kg^{-1}. [i] A_1 is constrained at 0.270 kg·mol^{-1}.

CO_2, O_2, Ar, *n*-butane, and light hydrocarbons, respectively.[22] There appears to be significant steric hindrance to the occupation of the total volume for small pore volume zeolites. Accordingly, in the calculation of q_s only 95% of the theoretical volume (110 cm^3·kg^{-1}) was considered to be available for occupancy at saturation.

In the constrained regression, the saturation concentrations for methane, ethane, and ethylene are fixed at (2.66, 1.75, and 2.00) mol·kg^{-1}, respectively. These values correspond to 95% of the theoretical values calculated from eq 5. Other model parameters exhibiting no trend in the unconstrained regression are optimized at a constant value intermediate between the minimum and maximum values obtained from the unconstrained regression corresponding to each parameter until a minimum sum-of-squares error is reached. The constrained regression results are given in Table 2 for methane, ethane, and ethylene.

As a result of constraining the model parameters, the total sum-of-squares error obtained from each model increases. However, the values of K_H become more consistent, with the exception of the K_H values for ethylene, which still exhibit a significant difference between the virial model and the models of Toth and unilan.

The van't Hoff equation parameters for the sorption of methane, ethane, and ethylene on titanosilicate ETS-10 zeolite are given in Table 3. The isosteric heat of adsorption parameters calculated for methane data using all models are consistent at approximately 21 kJ·mol^{-1}. Similarly, the preexponential factor K_o values are consistent at approximately 4.2×10^{-6} mol·kg^{-1}·kPa^{-1}.

Table 3. van't Hoff Sorption Parameters for Methane, Ethane, and Ethylene

model	$\sum$ss[a]	K_o/ 10^6mol·kg^{-1}·kPa^{-1}	$-\Delta H$/ kJ·mol^{-1}
	Methane		
Toth	0.3651	4.3810	21.445
unilan	0.2872	4.2356	21.049
virial three constant	0.1423	4.1354	20.784
	Ethane		
Toth	0.2028	0.9965	35.428
unilan	0.9712	1.5227	34.658
virial three constant	0.0966	0.9725	33.846
	Ethylene		
Toth	0.2722	1.2331	42.795
unilan	1.4121	4.7473	39.570
virial three constant	0.0014	5.0614	34.340

[a] Total sum of square error for all temperatures.

The values of the enthalpy of adsorption of Toth and unilan models for ethane data are comparable to the value obtained from the virial model at approximately 34 kJ·mol^{-1}. The preexponential factor for the Toth model approaches the value obtained for the virial three-constant model, but that for the unilan model is 50% larger.

The van't Hoff parameters obtained by all models for ethylene data deviate significantly from the values extracted for the virial three-constant model. This is attributed to the large deviation of Henry's constant values for these models.

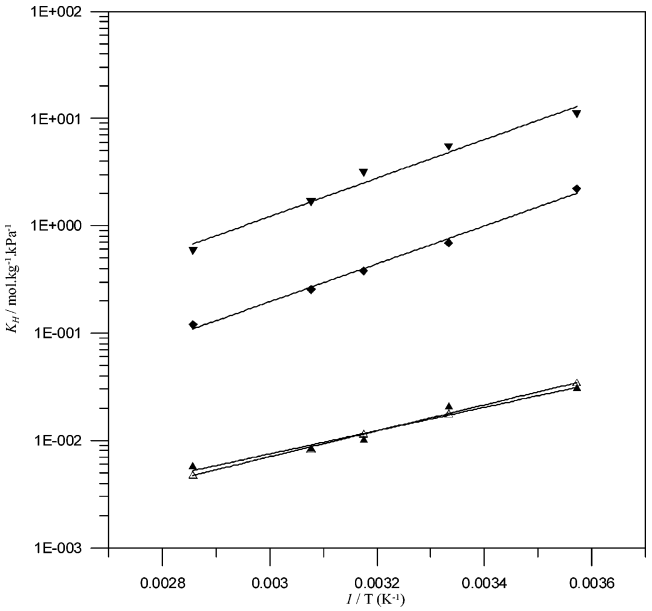

Figure 4. Arrhenius plot of Henry's constant values obtained from the virial three-constant model: ▲, methane; △, methane (Talu and Kuznicki[19]); ◆, ethane; ▼, ethylene.

Table 4. Comparison of Parameters for Virial Three-Constant Model

T/K	280	300	315	325	350
		This Work			
A_1/kg·mol^{-1}	0.550				
A_2/kg^2·mol^{-2}	0.000	0.225	0.283	0.195	0.519
A_3/kg^3·mol^{-3}	0.316	0.142	0.159	0.259	0.000
K_H/mol·kg^{-1}·kPa^{-1}	0.0306	0.0203	0.0100	0.0083	0.0057
$-\Delta H$/kJ·mol^{-1}	21.445				
		Calculated from Talu and Kuznicki[19]			
A_1/kg·mol^{-1}	0.301	0.369	0.414	0.442	0.505
A_2/kg^2·mol^{-2}	0.2212				
A_3/kg^3·mol^{-3}	0.0706				
K_H/mol·kg^{-1}·kPa^{-1}	0.0346	0.0179	0.0116	0.0084	0.0048
$-\Delta H$/kJ·mol^{-1}	22.938				

Plots of the isotherms of methane, ethane, and ethylene data on titanosilicate ETS-10 zeolite have been constructed together with the fit of the Toth, unilan, and virial three-constant models using the constrained parameters. The plots are shown in Figures 1, 2, and 3. The fit of the Arrhenius equation for the virial model is shown in Figure 4.

Detailed measurements in the literature for these systems on titanosilicate ETS-10 are scarce. The only study located is that of Talu and Kuznicki,[19] who studied the adsorption of methane on the same zeolite in the temperature range of 5 to 35 °C and pressure range 0 to 3447 kPa. They analyzed their system using the virial three-constant model with parameters A_i also as a function of temperature. Their calculated results are compared to this work in Table 4, and their calculated K_H values are also plotted in Figure 4 in the units employed in this study. The enthalpies of adsorption values differ by 6.96%. The K_H values plotted in Figure 4 reflect this difference but there is still remarkable agreement between both studies, as may be observed from the van't Hoff plot in Figure 4. The A_i values are similar, but there is a wider variation than for the other two parameters.

Conclusions

The fits of the three models (Toth, unilan, and virial) to the pure adsorption equilibrium data of methane, ethane, and ethylene on titanosilicate ETS-10 zeolite are excellent. The virial three-constant model appears to be the best model for deducing the true Henry's constant information. Using 95% of the theoretical value of the saturation concentrations improves the estimates of the Henry's constant in the Toth and unilan models. However, the Henry's constants of these models still differ slightly from the Henry's constants deduced from the virial model. This is a reflection of a numerical interaction between the Henry's constant and the saturation loading in optimizing these model parameters.

Acknowledgment

Acknowledgments are extended to S. M. Kusnicki of Engelhard who provided the samples of titanosilicate ETS-10 and to the Research Institute at KFUPM for assistance with the extrusion of the titanosilicate ETS-10 samples. We acknowledge the support of King Fahd University of Petroleum & Minerals (KFUPM), Dhahran, Saudi Arabia, during the course of this work.

Supporting Information Available:

Equilibrium adsorption data of methane on titanosilicate ETS-10 zeolite, ethane on titanosilicate ETS-10 zeolite, and ethylene on titanosilicate ETS-10 zeolite. This material is available free of charge via the Internet at http://pubs.acs.org.

Literature Cited

(1) Kuznicki, S. M.; Thrush, K. A.; Allen, F. M.; Levine, S. M.; Hamil, M. M.; Hayhurst, D. T.; Mansour, M. Synthesis and adsorptive properties of titanium silicate molecular sieves. *Synth. Microporous Mater*. **1992**, *1*, 427−456.

(2) Gervasini, A.; Carniti, P. CuO_x Siting on Titanium-Silicate (ETS-10): Influence of Copper Loading on Dispersion and Redox Properties in Relation with de-NO_x Activity. *Catal. Lett.* **2002**, *84*, 235−245.

(3) Gervasini, A.; Picciau, C.; Auroux, A. Characterization of Copper-exchanged ZSM-5 and ETS-10 Catalysts with Low and High degrees of Exchange. *Microporous Mesoporous Mater.* **2000**, *457*, 35−36.

(4) Bianchi, C. L.; Carli, R. ETS-10 Titanium Silicate Catalysts. *Catal. Lett.* **1996**, *41*, 79−82.

(5) Bianchi, C. L.; Vitali, S.; Ragaini, V. Comparison Between Co And Co (Ru−Promoted)-ETS-10 Catalysts Prepared In Different Ways For Fischer−Tropsch Synthesis. *Stud. Surf. Sci. Catal.* **1998**, *119*, 167−172.

(6) Carniti, P.; Gervasini, A.; Auroux, A. Copper Site Energy Distribution of de-NO_x Catalysts Based on Titanosilicate (ETS-10). *Langmuir* **2001**, *17*, 6938−6945.

(7) Pavel, C. C.; Vuono, D.; Nastro, A.; Nagy, J. B.; Bilba, N. Synthesis and Ion Exchange Properties of the ETS-4 and ETS-10 Microporous Crystalline Titanosilicates. *Stud. Surf. Sci. Catal.* **2002**, *142A*, 295−302.

(8) Pavel, C. C.; Vuono, D.; Catanzaro, L.; De Luca, P.; Bilba, N.; Nastro, A.; Nagy, J. B. Synthesis and Characterization of the Microporous Titanosilicates ETS-4 and ETS-10. *Microporous Mesoporous Mater.* **2002**, *56*, 227−239.

(9) Zibrowius, B.; Weidenthaler, C.; Schmidt, W. Sorbate-Induced Changes in the Framework of ETS-10 as Detected by Si MAS NMR Spectroscopy and X-ray Powder Diffraction. *Phys. Chem. Chem. Phys* **2003**, *5*, 773−777.

(10) Otero Areán, C.; Turnes Palomino, G.; Zecchina, A.; Bordiga, S.; Llabrés, I.; Xamena, F. X.; and Pazè, C. Vibrational Spectroscopy of Carbon Monoxide and Dinitrogen Adsorbed on Magnesium Exchanged ETS-10 Molecular Sieve. *Catal. Lett.* **2000**, *66*, 231−235.

(11) Anderson, M. W.; Agger, J. R.; Luigi, D. P.; Baggaley, A. K.; Rocha, J. Cation Sites in ETS-10: Na-23 3Q MAS NMR and Lattice Energy Minimization Calculations. *Phys. Chem. Chem. Phys.* **1999**, *1*, 2287−2292.

(12) Grillo, M.; Carrazza, J. Computational Modeling of the Nonframework Cation Location and Distribution in Microporous Titanosilicate ETS-10. *J. Phys. Chem.* **1996**, *100*, 122−161.

(13) Grillo, M. E.; Carazza, J. Computer Simulation Study of the Microporous Titanosilicate ETS-10. *J. Phys. Chem. B* **1997**, *101*, 6749−6752.

(14) Yang, X.; Truitt, R. E. NMR Investigation of ETS-10. *J. Phys. Chem.* **1996**, *100*, 3713−3719.

(15) Kishima, M.; Okubo, T. Characterization of Microporous Titanosilicate ETS-10 by Infrared Spectroscopy with Methane as a Probe Molecule for Basic Sites. *J. Phys. Chem. B* **2003**, *107*, 8462−8468.
(16) Sankar, G.; Bell, R. G.; Thomas, J. M.; Anderson, M. W.; Wright, P. A.; Rocha, J. Determination of the Structure of Distorted TiO_6 Units in the Titanosilicate ETS-10 by a Combination of X-ray-Absorption Spectroscopy and Computer Modeling. *J. Phys. Chem.* **1996**, *100*, 449−452.
(17) Ashtekar, S.; Prakash, A. M.; Kevan, L.; Gladden, L. F. Sorbate-Framework Interactions as an Aid to Vibrational Mode Assignment: FT-Raman Studies of ETS-10. *Chem. Commun.* **1998**, *1*, 91−92.
(18) Zecchina, A.; Otero Arean, C.; Turnes Palomino, G.; Geobaldo, F.; Lamberti, C.; Spoto, G.; Bordiga, S. The Vibrational Spectroscopy of H_2, N_2, CO and NO Adsorbed on the Titanosilicate Molecular Sieve ETS-10. *Phys. Chem. Chem. Phys.* **1999**, *1*, 1649−1657.
(19) Talu, O.; Kuznicki, S. M. Pure Component Adsorption on ETS-10. Fundamentals of Adsorption: FOA6, Giens, France, May 24−28, 1998.
(20) Kishima, M.; Okubo, T. Characterization of Basic Sites by Infrared Spectroscopy Using Methane as a Probe Molecule. *Zeoraito* **2003**, *20*, 41−46.
(21) Kuznicki, S. M.; Bell, V. A.; Nair, S.; Hillhouse, H. W.; Jacubinas, R. M.; Braunbarth, C. M.; Toby, B. H.; Tsapatsi, M. A Titanosilicate Molecular Sieve with Adjustable Pores for Size-Selective Adsorption of Molecules. *Nature* **2001**, *412*, 720−724.
(22) Breck, D. W. *Zeolite Molecular Sieves*; Wiley: New York, 1974.
(23) Dubinin, M. M. Adsorption Properties and Secondary Pore Structure of Adsorbents that Exhibit Molecular-Sieve Action. II. Comparison of Calculated and experimental Limiting Values for Adsorption and Adsorption Volumes for Type A Synthetic Zeolites. *Izv. Akad. Nauk, Ser. Khim.* **1961**, 1183−1191.
(24) Al-Baghli, N. Adsorption of Light Gases and Their Mixtures on Sr-115 and ETS-10 Zeolites: M.S. Thesis, King Fahd University of Petroleum & Minerals, Dhahran, Saudi Arabia, 1994.
(25) Toth, J. State Equations of the Solid−Gas Interface Layers. *Acta Chim. Acad. Sci. Hung.* **1971**, *69*, 311−328.
(26) Honig, J. M.; Reyerson, L. H. Adsorption of Nitrogen, Oxygen, and Argon on Rutile at Low Temperatures; Applicability of the Concept of Surface Heterogeneity. *J. Phys. Chem*. **1952**, *56*, 140−146.
(27) Barrer, R. M. *Zeolites and Clay Minerals as Sorbents and Molecular Sieves*. Academic Press: London, 1978.
(28) Kuznicki, S. M. Personal communication, 1993.
(29) Abdul Rehman, H. Equilibrium Adsorption of Light Gases and Their Mixtures on 5A, 13X, and SR-115: M.S. Thesis, King Fahd University of Petroleum & Minerals, Dhahran, Saudi Arabia, 1984.
(30) Abdul-Rehman, H. B.; Hasanain, M. A.; Loughlin, K. F. Quaternary, Ternary, Binary, and Pure Component Sorption on Zeolites. 1. Light Alkanes on Linde S-115 Silicalite at Moderate to High Pressures. *Ind. Eng. Chem. Res*. **1990**, *29*, 1525−1535.

Received for review September 5, 2004. Accepted March 10, 2005.

JE0496793